Orbital Kondo Effect in Cobalt-Benzene Sandwich Molecules

M. Karolak,[1] D. Jacob,[2] and A. I. Lichtenstein[1]

[1]*I. Institut für Theoretische Physik, Universität Hamburg, Jungiusstraße 9, D-20355 Hamburg, Germany*
[2]*Max-Planck-Institut für Mikrostrukturphysik, Weinberg 2, 06120 Halle, Germany*

(Received 24 May 2011; published 30 September 2011)

We study a Co-benzene sandwich molecule bridging the tips of a Cu nanocontact as a realistic model of correlated molecular transport. To this end we employ a recently developed method for calculating the correlated electronic structure and transport properties of nanoscopic conductors. When the molecule is slightly compressed by the tips of the nanocontact the dynamic correlations originating from the strongly interacting Co 3*d* shell give rise to an orbital Kondo effect while the usual spin Kondo effect is suppressed due to Hund's rule coupling. This nontrivial Kondo effect produces a sharp and temperature-dependent Abrikosov-Suhl resonance in the spectral function at the Fermi level and a corresponding Fano line shape in the low bias conductance.

DOI: 10.1103/PhysRevLett.107.146604 PACS numbers: 72.15.Qm, 31.15.A−, 71.27.+a, 73.63.Rt

The discovery of ferrocene and bisbenzene chromium [1] over half a century ago was the starting point for experimental and theoretical work both in chemistry and physics concerning the intricate properties of organometallic compounds. The investigation of these and related sandwich complexes is driven by their relevance in various chemical applications (e.g., catalysis) and, more recently, because of their prospective nanotechnological applications, for example, as molecular magnets [2] or spintronic devices [3].

Molecules with a transition metal (TM) center coupled to aromatic groups are also of high interest from a fundamental point of view. The strong electronic correlations in the *d* shell of the TM can modify the ground state and electronic transport properties of such molecules, leading to many-body phenomena like the Kondo effect [4] as recently observed in TM-phthalocyanine molecules [5]. The importance of dynamical correlations in nanoscopic devices in general is further substantiated by the recent observation of the Kondo effect in nanocontacts made from TMs [6,7]. Also recently, a so-called underscreened Kondo effect has been reported for a molecule trapped in a break-junction [8]. While the Kondo effect is commonly associated with the screening of a local magnetic moment by the conduction electrons, it is also possible that another internal degree of freedom associated with a degeneracy gives rise to a Kondo effect [9]. One example is the so-called orbital Kondo effect where the pseudospin arising from an orbital degeneracy is screened by the conduction electrons [10].

Such complex many-body phenomena call for a theoretical description beyond the standard treatment with Kohn-Sham (KS) density functional theory (DFT) which cannot capture many-body physics beyond the effective mean-field picture. The incorrect behavior of the KS DFT for strongly correlated systems can be remedied by augmenting the DFT with a local Hubbard-like interaction. This DFT + + approach is the de facto standard in the theory of solids [11]. Recently this approach has been adapted to the case of nanoscopic conductors [7,12,13].

In this letter we apply this method to investigate the transport properties of cobalt-benzene sandwich molecules $(C_6H_6)Co(C_6H_6)$ ($CoBz_2$ in the following). We find that dynamical correlations in the Co 3*d* shell give rise to an orbital Kondo effect in a doubly-degenerate level of the Co 3*d* shell while the usual spin Kondo effect is suppressed due to Hund's rule coupling.

We perform DFT calculations using the CRYSTAL06 code [14] employing the local density approximation (LDA) [15], PW91 [16], and the hybrid functional B3LYP [17], and using the all electron Gaussian 6–31 G basis set. The geometries of the wires were relaxed beforehand and kept fixed during the calculations. The geometry of the molecule in contact with the wires was relaxed, employing the B3LYP functional [18].

In order to capture many-body effects beyond the DFT level, we have applied the DFT + OCA (density functional theory plus one-crossing approximation) for nanoscopic conductors developed by one of us in earlier work [7,12]. To this end the system is divided into three parts: The two semi-infinite leads *L* and *R* and the device region *D* containing the molecule and part of the leads. The KS Green's function (GF) of region *D* can now be obtained from the DFT electronic structure as $G_D^0(\omega) = [\omega + \mu - H_D^0 - \Sigma_L(\omega) - \Sigma_R(\omega)]^{-1}$ where H_D^0 is the KS Hamiltonian of region *D* and $\Sigma_{L,R}(\omega)$ are the so-called lead self-energies which describe the coupling of *D* to *L* and *R* and which are obtained from the DFT electronic structure of the nanowire leads.

Next, the mean-field KS Hamiltonian is augmented by a Hubbard-like interaction term $\sum_{ijkl} U_{ijkl} \hat{d}_i^\dagger \hat{d}_j^\dagger \hat{d}_l \hat{d}_k$ that accounts for the strongly interacting electrons of the Co 3*d* shell. Here we use a simplified interaction which only takes into account the direct Coulomb repulsion $U \equiv U_{ijij}$ and the

Hund's rule coupling $J \equiv U_{ijji}$. These are different from the bare interactions due to screening processes. Here we assume that the interactions are somewhat increased as compared to their bulk values since the screening should be weaker than in bulk. Hence, we use $U = 5$ eV and $J = 1$ eV; indeed, we find that our results are qualitatively stable for a reasonable range of values for U and J (see below).

The interacting Co $3d$ shell coupled to the rest of the system (benzene + leads) constitutes a so-called Anderson impurity model (AIM). The AIM is completely defined by the interaction parameters U and J, the energy levels ϵ_d of the $3d$ orbitals, and the so-called hybridization function $\Delta_d(\omega)$. The latter describes the (dynamic) coupling of the Co $3d$ shell to the rest of the system and can be obtained from the KS GF as $\Delta_d(\omega) = \omega + \mu - \epsilon_d^0 - [G_d^0(\omega)]^{-1}$ where μ is the chemical potential, ϵ_d^0 are the KS energy levels of the $3d$ orbitals, and $G_d^0(\omega)$ is the KS GF projected onto the $3d$ subspace. The energy levels ϵ_d are obtained from the static crystal field ϵ_d^0 where, as usual, in DFT + + approaches a double counting correction (DCC) has to be subtracted to compensate for the overcounting of interaction terms. Here we employ the so-called fully localized or atomic limit DCC [19] $E_{dc} = U \cdot (N_{3d} - \frac{1}{2}) - J(\frac{N_{3d}}{2} - \frac{1}{2})$.

The AIM is solved within the OCA [11,20]. This yields the electronic self-energy $\Sigma_d(\omega)$ which accounts for the electronic correlations of the $3d$-electrons due to strong electron-electron interactions. The correlated $3d$ GF is then given by $G_d = [(G_d^0)^{-1} - \Sigma_d + E_{dc}]^{-1}$. Correspondingly, the correlated GF for D is given by $G_D = [(G_D^0)^{-1} - \Sigma_d + E_{dc}]^{-1}$ where Σ_d and E_{dc} only act within the $3d$ subspace. From G_D we can calculate the transmission function $T(\omega) = \mathrm{Tr}(\Gamma_L G_D^\dagger \Gamma_R G_D)$ where $\Gamma_\alpha \equiv i(\Sigma_\alpha - \Sigma_\alpha^\dagger)$. For small bias voltages V, the transmission yields the conductance: $\mathcal{G}(V) = (2e^2/h)T(eV)$.

We consider a single $CoBz_2$ molecule in contact with two semi-infinite Cu nanowires as shown in Fig. 1(a). The $CoBz_2$ molecule is the smallest instance of a general class of M_nBz_{n+1} complexes, where M stands for a metal atom, that have been prepared and investigated [3,21]. The semi-infinite Cu wires exhibit the hexagonal symmetry of the molecule and correspond to the (6,0) wires described in Ref. [22]. We investigate the system at three different Cu-tip-Co distances 3.6 Å, 4.0 Å, and 4.3 Å [see Figs. 1(a) and 1(b)]. As can be seen from Fig. 1(b) the Bz-Bz distance h varies between 3.4 Å and 3.65 Å depending on the distance d of the Cu tip to the Co atom in the center of the molecule. At distances $d = 3.6$ Å and $d = 4.0$ Å the molecule is slightly compressed compared to its free height of about $h = 3.6$ Å, whereas it is slightly stretched at $d = 4.3$ Å.

The hexagonal symmetry of the system leads to a lifting of the degeneracy of the five $3d$ orbitals. The symmetry adapted representations are: the A_1 group, consisting of the $d_{3z^2-r^2}$ orbital only, the doubly degenerate E_1 group, consisting of the d_{xz} and d_{yz} orbitals, and the E_2 group, consisting of the d_{xy} and $d_{x^2-y^2}$ orbitals.

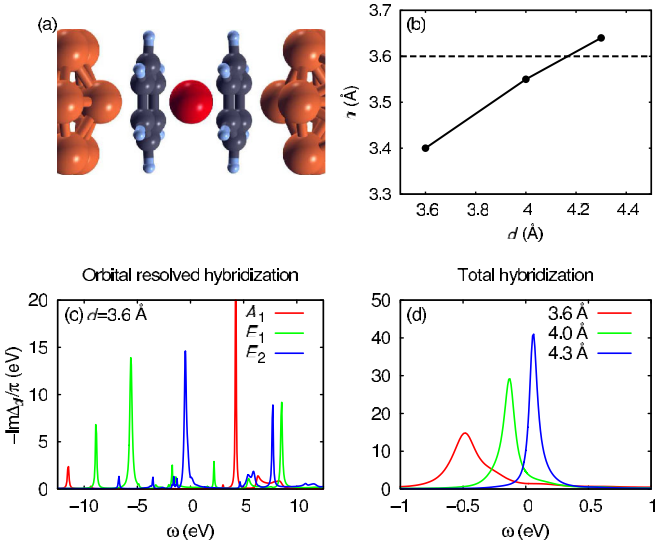

FIG. 1 (color online). (a) Atomic structure of the $CoBz_2$ molecule in a Cu nanocontact. (b) Size h of the $CoBz_2$ molecule as a function of the distance d between a Co atom and Cu tip atoms. (c) Orbitally resolved imaginary part of the hybridization function for $d = 3.6$ Å. (d) Total hybridization function (all Co $3d$ orbitals) for different d.

Figures 1(c) and 1(d) show the imaginary parts of the hybridization functions $\Delta_d(\omega)$ calculated from the LDA electronic structure. The imaginary part of the hybridization function exhibits a distinct peak close to the Fermi level (E_F) in the E_2 channel, whose position, width, and height depend significantly on the molecular geometry, specifically on the Bz-Co distance. The other channels E_1 and A_1 show only a negligible hybridization close to E_F. The dominant feature stems, similarly as shown for graphene [12,23] from hybridization with the π_z orbital state of the benzene rings. The feature does not depend qualitatively on the DFT functional used, as we have found the same feature within the generalized gradient approximation and also in B3LYP calculations. The presence of strong molecular resonances in the hybridization function makes this case different from the case of nanocontacts with magnetic impurities where the hybridization functions are generally much smoother (see Ref. [7] for comparison).

Figure 2(a) compares the correlated spectral functions $A_d(\omega) \sim \mathrm{Im}G_d$ of the Co $3d$ electrons for the three distances considered here at high temperatures on a large energy scale. The spectra vary considerably as the distance d changes. Most important, for d around 3.6 Å when the molecule is slightly compressed, a sharp temperature-dependent peak appears right at E_F, as can be seen from Fig. 2(b). The peak is strongly renormalized (i.e., it only carries a small fraction of the spectral weight) due to the strong electron-electron interactions.

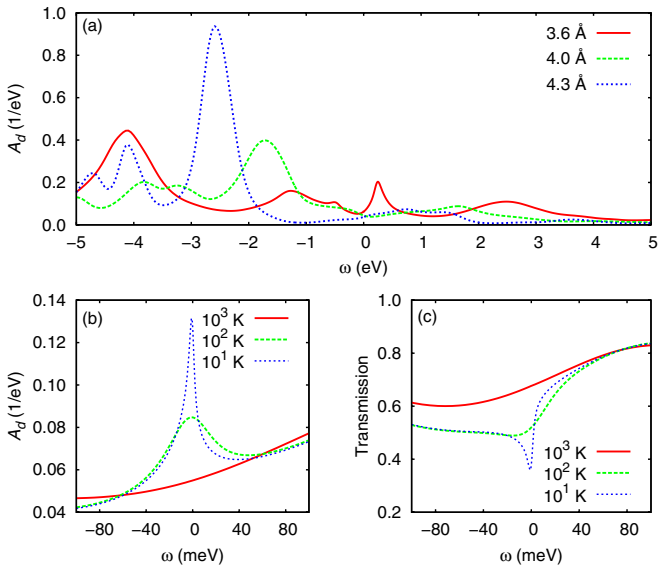

FIG. 2 (color online). (a) Spectral functions of the Co 3d shell for different d at temperature $T \sim 1200$ K. (b), (c) Spectral and transmission functions of the molecule at $d = 3.6$ Å for different temperatures.

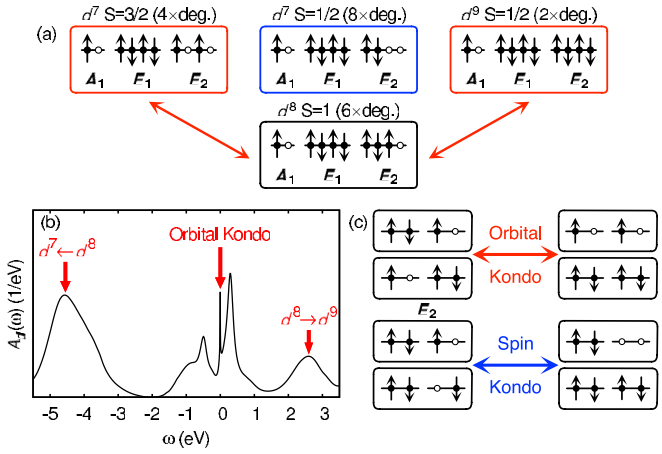

FIG. 3 (color online). (a) Fluctuations between the atomic states that give rise to the spectral features shown in (b). (b) Spectral function around E_F for $d = 3.6$ Å. Arrows indicate spectral features arising from the fluctuations between atomic states shown in (a). (c) Orbital and spin flip fluctuations in the E_2 channel that can lead to an orbital Kondo effect and to an underscreened spin Kondo effect, respectively.

The sharp peak in the spectral function at E_F that starts to develop already at temperatures of $kT = 0.01$ eV $\approx$ 120 K stems from the E_2 channel which is the only channel with appreciable hybridization near E_F; see Figs. 1(b) and 1(c). Correspondingly, the transmission function [Fig. 2(c)] shows a Fano-like feature around zero energy. A renormalized, sharp, and temperature-dependent resonance in the spectral function at E_F is commonly associated with the Kondo effect. Looking at the orbital occupations, we find that the E_2 channel that gives rise to the resonance for $d = 3.6$ Å has an occupation of about 2.8 while the total occupation of the 3d shell is $N_d \sim 7.5$. The fractional occupation numbers indicate the presence of valence fluctuations where the charges in the individual impurity levels fluctuate in contrast to the pure Kondo regime where these fluctuations are frozen.

Analyzing the atomic states of the Co 3d shell contributing to the ground state of the system we find that the principal contribution ($\sim 45\%$) is an atomic state with 8 electrons and a total spin of $S = 1$ (d^8, $S = 1$) as shown in Fig. 3(a). The total spin 1 stems from holes in the E_2 and A_1 channels. The charge fluctuations in the E_2 channel are mainly due to the contribution ($\sim 17\%$) of an atomic (d^7, $S = 3/2$) state. There are considerably weaker contributions ($\sim 4\%$) from atomic (d^7, $S = 1/2$) and (d^9, $S = 1/2$) states. The individual contributions of the remaining atomic states are very small (below 1%) but add up to a total contribution of 34%.

By exclusion of individual atomic states from the calculation of the spectra we can determine which fluctuations are responsible for the different spectral features. We find that the fluctuations between the (d^8, $S = 1$) and the (d^7, $S = 3/2$) states are primarily responsible for the three spectral features close to E_F including the sharp Kondo-like peak right at E_F, as illustrated in Fig. 3(b). Also, the broad peak around 4 eV below E_F originates from these fluctuations while the broad peak that is about 2.5 eV above E_F arises from fluctuations between the (d^9, $S = 1/2$) atomic state and the principal d^8 atomic state. The two peaks in the spectral function nearest to the Kondo resonance arise from the strong energy dependence of the hybridization function whose real part has poles just below and above E_F roughly at the positions of these two spectral features.

Note that the fluctuations from the (d^8, $S = 1$) to the (d^7, $S = 3/2$) states that give rise to the Kondo-like peak at E_F actually cannot lead to a spin Kondo effect since the spin 3/2 of the d^7 state is higher than the spin 1 of the principal d^8 state. Instead, the fluctuations between the (d^8, $S = 1$) and the (d^7, $S = 3/2$) states which give rise to the Kondo-like resonance at E_F correspond to an orbital Kondo effect in the doubly degenerate E_2 levels of the Co 3d shell as illustrated in the upper panel of Fig. 3(c). Here the index labeling the two orbitals with E_2 symmetry takes over the role of a pseudospin. In the principal d^8 atomic state the E_2 levels are occupied with three electrons and hence have a pseudospin of 1/2. By excitation to the (d^7, $S = 3/2$) state the electron with minority real spin and with some pseudospin state is annihilated. By relaxation to the principal electronic (d^8, $S = 1$) state a minority real spin electron can now be created in one of the two pseudospin states. Those processes that lead to a flip of the pseudospin then give rise to the orbital Kondo effect and the formation of the Kondo peak at E_F.

The absence of a normal spin Kondo effect, where the total spin 1 of the principal d^8 atomic state is screened, is easily understood on the following grounds: In general, the Kondo scale decreases exponentially with increasing spin of the magnetic impurity [24]. In addition, here the A_1 level does not couple at all to the conduction electrons around E_F (no hybridization). Thus, the spin $1/2$ associated with it cannot be flipped directly through hopping processes with the conduction electron bath.

On the other hand, an underscreened Kondo effect, as reported in Ref. [8] where only the spin $1/2$ within the E_2 shell is screened, is also suppressed compared to the orbital Kondo effect due to Hund's rule coupling: Screening of the spin $1/2$ in the E_2 shell can take place by fluctuations to the (d^7, $S = 1/2$) state. However, the Hund's rule coupling J favors the high spin (d^7, $S = 3/2$) state over the low spin (d^7, $S = 1/2$) state as can also be seen from the smaller weight of the latter compared to the former. Hence, the Kondo scale is considerably lower for the underscreened Kondo effect than for the orbital Kondo effect found here. At lower temperatures (not accessible with OCA) the two Kondo effects may in fact coexist.

We have also checked the dependence of the LDA + OCA spectra on the DCC as well as on the interaction parameters U and J (not shown [25]). In general we find the spectra and also the Kondo peak to be qualitatively robust against shifts of the impurity levels in energy over a range of several electron volts, and changes of U between 3 and 7 eV, and of J between 0.6 to 1 eV. As expected for the Kondo effect the sharp resonance stays pinned to the Fermi level when shifting the impurity levels in energy, and only height and width somewhat change.

Stretching the molecule by displacing the tips of the Cu nanowires the Kondo resonance and the concomitant Fano line shape in the transmission disappear for distances $d \geq 4$ Å (not shown). This is accompanied by an increase of the occupation of the Co $3d$ shell. The new regime is characterized by a strong valence mixing between the d^8 and d^9 atomic states of roughly equal contribution indicating that the system is now in the so-called mixed valence regime (see, e.g., Ref. [4], chap. 5). Hence, the orbital Kondo effect and the associated spectral features can be controlled by stretching or compressing the molecule via the tip atoms of the Cu nanocontact. This strong sensitivity on the molecular conformation stems from the sharp features in the hybridization function which change considerably when the molecule is stretched or compressed, as can be seen from Fig. 1(d). This peculiar behavior is qualitatively different from the case of the nanocontacts containing magnetic impurities where the hybridization functions are much smoother [7].

In conclusion, we have shown for a $CoBz_2$ sandwich molecule coupled to Cu nanowires that the dynamic correlations originating from the strongly interacting Co $3d$ electrons give rise to an orbital Kondo effect in the doubly degenerate E_2 levels while a spin Kondo effect is suppressed by Hund's rule coupling. Because of the sensitivity of the electronic correlations on the molecular conformation it is possible to control the appearance of the orbital Kondo effect by stretching and compressing the molecule with the tips of the Cu leads. It should be possible to prepare a setup similar to the one considered here in an actual experiment and measure the orbital Kondo effect, e.g., by contacting a $CoBz_2$ molecule deposited on a Cu(111) surface with a scanning tunneling microscope. Finally, we mention that we have also explored the case of a $NiBz_2$ sandwich. In this case we do not find a Kondo effect. Instead the system is in the mixed valence regime characterized by a strong peak with weak temperature dependence close to, but not at E_F [25].

We thank K. Haule for providing us with the OCA impurity solver and for helpful discussions. Support from SFB 668, LEXI Hamburg and ETSF are acknowledged. M. K. gratefully acknowledges the hospitality of the Max-Planck-Institute in Halle (Saale).

[1] T. Kealy and P. Pauson, Nature (London) **168**, 1039 (1951); E. Fischer and W. Hafner, Z. Naturforsch. B **10**, 665 (1955).
[2] D. Gatteschi, R. Sessoli, and J. Villain, *Molecular Nanomagnets* (Oxford University Press, Oxford, 2006).
[3] H. Xiang *et al.*, J. Am. Chem. Soc. **128**, 2310 (2006); Y. Mokrousov *et al.*, Nanotechnology **18**, 495402 (2007).
[4] A. C. Hewson, *The Kondo Problem to Heavy Fermions* (Cambridge University Press, Cambridge, 1997).
[5] A. Zhao *et al.*, Science **309**, 1542 (2005); L. Gao *et al.*, Phys. Rev. Lett. **99**, 106402 (2007).
[6] M. R. Calvo *et al.*, Nature (London) **458**, 1150 (2009).
[7] D. Jacob, K. Haule, and G. Kotliar, Phys. Rev. Lett. **103**, 016803 (2009).
[8] J. J. Parks *et al.*, Science **328**, 1370 (2010).
[9] D. L. Cox and A. Zawadowski, Adv. Phys. **47**, 599 (1998).
[10] O. Y. Kolesnychenko *et al.*, Nature (London) **415**, 507 (2002); Jarillo-Herrero *et al.*, *ibid.* **434**, 484 (2005).
[11] G. Kotliar *et al.*, Rev. Mod. Phys. **78**, 865 (2006); A. I. Lichtenstein and M. I. Katsnelson, Phys. Rev. B **57**, 6884 (1998).
[12] D. Jacob and G. Kotliar, Phys. Rev. B **82**, 085423 (2010); D. Jacob, K. Haule, and G. Kotliar, *ibid.* **82**, 195115 (2010).
[13] P. Lucignano *et al.*, Nature Mater. **8**, 563 (2009); L. G. G. V. Dias da Silva *et al.*, Phys. Rev. B **80**, 155443 (2009); R. Korytár and N. Lorente, arXiv:1102.1667v1; A. Valli *et al.*, Phys. Rev. Lett. **104**, 246402 (2010).
[14] R. Dovesi *et al.*, CRYSTAL06, Release 1.0.2, Theoretical Chemistry Group, Universita' Di Torino, Torino (Italy).
[15] W. Kohn and L. J. Sham, Phys. Rev. **140**, A1133 (1965).
[16] J. P. Perdew and Y. Wang, Phys. Rev. B **33**, 8800 (1986).
[17] A. D. Becke, J. Chem. Phys. **98**, 5648 (1993).
[18] Although for the free molecule the two benzene rings tilt toward each other [21], we find that the presence of the

electrodes stabilizes the linear geometry considered here. See the Supplemental Material for details [25].
[19] M. T. Czyżyk and G. A. Sawatzky, Phys. Rev. B **49**, 14211 (1994).
[20] K. Haule *et al.*, Phys. Rev. B **64**, 155111 (2001).
[21] T. Kurikawa *et al.*, Organometallics **18**, 1430 (1999); A. Nakajima and K. Kaya, J. Phys. Chem. A **104**, 176 (2000); J. Martinez *et al.*, J. Chem. Phys. **132**, 044314 (2010); X. Zhang and J. Wang, J. Phys. Chem. A **112**, 296 (2008).
[22] E. Tosatti *et al.*, Science **291**, 288 (2001).
[23] T. O. Wehling *et al.*, Phys. Rev. B **81**, 115427 (2010).
[24] A. H. Nevidomskyy and P. Coleman, Phys. Rev. Lett. **103**, 147205 (2009).
[25] See Supplemental Material at http://link.aps.org/supplemental/10.1103/PhysRevLett.107.146604 for information on the influence of the electrodes on the geometry of the molecule, the dependence of the LDA + OCA results on the parameters of the calculation, and preliminary results on $NiBz_2$.